Al-Kitab Journal for Pure Sciences (2023); 7(2):16-29.
https://doi.org/10.32441/kjps.07.02.p2

Al-Kitab Journal for Pure Sciences
ISSN: 2617-1260 (print), 2617-8141(online)

https://isnra.net/index.php/kjps

Study of the optical and spectral properties of Phosphor Tellurite Semiconducting Oxide Glasses

Hazhar.Kh.Omer*, Manaf.A.Hassan

Department of physics, faculty of education of pure sciences, University of Kirkuk, Kirkuk, Iraq

*Corresponding Author: hazharkhalid515@gmail.com

Citation: Omer HKH, Hassan MA. Study of the optical and spectral properties of Phosphor Tellurite Semiconducting Oxide Glasses. Al-Kitab J. Pure Sci. [Internet]. 2023 Sep. 10 [cited 2023 Sep. 10];7(2):16-29. https://isnra.net/index.php/kjps/article/view/951. https://doi.org/10.32441/kjps.07.02.p2.

Keywords: Optical energy gap. Urbach energy, X-ray, SEM, Glass system, DSC.

Article History

Received	20 July.	2023
Accepted	15 Aug.	2023
Available online	10 Sep.	2023

Abstract:

A systematic series of binary Phosphor tellurite glasses in the form [(90-X%)TeO2-(X%)V2O5] in mol%, where X = (10,20,25,30,35) have been successfully prepared in standard method (melt quenching), The effect of adding (V2O5) have been discussed. The X-Ray diffraction spectrum shows that the glass composite had no sharp peaks, The absence of abroad hump at (2θ=25-30o) indicates the presence of (L.R.O) long-range structural was disorder. The glass network structure was discussed through IR and Raman spectroscope and that showed the glass network is built of (TeO3 and TeO4) units. From the UV-visible spectrum, the edge of absorption the optical energy gap (Eopt) Urbach energy (Eo), and refractive index (n), have been determined. The results show that (Eopt) decreased with the increase of (V2O5) concentration, and Urbach energy (Eo) decreased with the increase of (V2O5) content, the refractive index (n) increased with the increase of (V2O5) concentration. The thermal parameters such as transition temperature (Tg), thermal stability (S), and thermodynamic fragility (F) are calculated by differential scanning calorimetry (DSC). Structural analysis of the glass system was identified by scanning electron microscopy (SEM).

Keywords: Optical energy gap. Urbach energy, X-Ray, SEM, Glass system, DSC.

دراسة الخصائص البصرية والطيفية لزجاجيات أوكسيد الفوسفور والتيليريوم الشبه الموصلة

ههژار خالد عمر*، مناف عبد حسن

جامعة كركوك كلية التربية للعلوم الصرفة–قسم الفيزياء، العراق
hazharkhalid515@gmail.com

الخلاصة:

تم تحضير سلسلة من عينات الزجاجية شبه الموصلة من أوكسيد التيليريوم الثنائي و أوكسيد الفوسفور الخماسي حسب المعادلة $[X)$ %(90-[TeO_2-(X)%V_2O_5 حيث قيم $(X = (10□20□25□30□35$ حيث تم تحضيرها بنجاح باستخدام الطريقة التقليدية في تحضير الزجاج (التبريد بالذوبان)، وتمت مناقشة تأثير إضافة (V_2O_5) ويبين طيف حيود الأشعة السينية أن المركب الزجاجي لا يحتوي على قمم حادة، ويشير وجود هالة عريضة عند (θ=25-30o٢) إلى عدم وجود ترتيب بنيوي طويل المدى.(*LRO*) كذلك تمت مناقشة بنية الشبكة الزجاجية من خلال مطيافية الأشعة تحت الحمراء و مطيافية رامان والتي أظهرت أن الشبكة الزجاجية متكونة من وحدات (TeO_3 & TeO_4)، ومن خلال الطيف المرئي للأشعة فوق البنفسجية تم تحديد حافة الامتصاص البصري وفجوة الطاقة الضوئية (E_{opt}) وطاقة اورباخ (E_o) ومعامل الانكسار(n))، وأظهرت النتائج أن قيم (E_{opt}) تنخفض مع الزيادة في تركيز (V_2O_5) وقيم (E_o) أيضاً، ومع الزيادة في تركيز (V_2O_5) نلاحظ ازدياداً في قيم معامل الانكسار(n)، المعاملات الحرارية مثل درجة حرارة الانتقال الزجاجيT_g ، والاستقرار الحراري S والهشاشة الثرمودياناميكيةF المقاسة عن طريق المسعر الحراري التفاضلي(*DSC*)، وتم التعرف على التحليل التركيبي للنظام الزجاجي عن طريق المسح المجهري الإلكتروني(*SEM*).

الكلمات المفتاحية: فجوة الطاقة البصرية، طاقة اورباخ، حيود الأشعة السينية، المجهر الماسح الإلكتروني، المسعر الحراري التفاضلي.

1. INTRODUCTION:

Specific optical properties make this glass particularly suitable for equipment in different laboratories [1]. Tellurium-containing glass melts quickly and is therefore considered a promising material due to its optical properties [2]. Transition materials have been used because they have more than two valence states that affect the optical parameters of the glass [3,4]. Vanadium pentoxide (V2O5) doped with a divalent ratio of {V+4/V+5} is an n-type semiconductor [5]. Tellurite glasses have gained importance in the optical instrumentation industry due to their high transparency in the visible and infrared spectrum [6]. The topology of tellurium-containing glasses is based on the presence of different types of TeO4 and TeO3 units [7]. The structural and optical properties of tellurite glasses have been studied [9,10,11,]. Glasses can be formed when tellurium dioxide (TeO2) is mixed with many different oxides from groups III, IV, and V of the periodic table. The triangular bipyramid (TeO4) transforms into (TeO3) and forms an alkali metal oxide [8]. Tellurium dioxide-based glasses have weak Te-O bonds that are easily broken and are therefore suitable for accommodating metal oxide ions [9]. This study aimed to investigate the effect of (V2O5) on the optical, thermal, and structural properties of tellurite glass systems.

2. Experimental work

Ternary glasses of the type [(90-X%)TeO2-(X%)V2O5] were prepared from (V2O5-TeO2) by use of the standard (melt-quenching) technique. The appropriate amounts of reagents were mixed in alumina crucibles in an electric furnace kept at (850-950Co). then the series of melts was poured on the stainless plate at 450 Co The glass samples had a thickness (1mm). The structure of the glasses was checked by X-ray diffraction (XRD) using (PANalytical) radiation. Scanning electron microscopy (SEM) measured by (KYKYEM3200) images were acquired from the surfaces of glass samples. The IR and Raman spectroscopy of the glass system was recorded at room temperature in the 400-4000 cm-1 wave number range. The optical properties measurements by (UV-Visible-Biomte5) with wavelength range from 100-900nm. Thermal parameters investigated by (DSC) were glass transition temperature (Tg), thermal stability (S) and thermodynamic fragility (F) have been calculated.

3. Results and discussion

3.1 X-ray diffraction

X-ray diffraction spectra of (TeO_2-V_2O_5) glass samples were recorded at an angle of 2° in the range of 80° ≥ ϴ ≥ 10°. **Figure (1)** shows that the XRD spectrum has no discrete or continuous peaks. The absence of sharp peaks and hillocks at (~27o) indicates the presence of long-range structural faults [10]. Since no sharp line spectrum was obtained in the XRD spectrum, it can be assumed that there is no evidence of a crystalline phase in the glass sample. The broad hump pattern indicates that the as-prepared glass samples are amorphous.

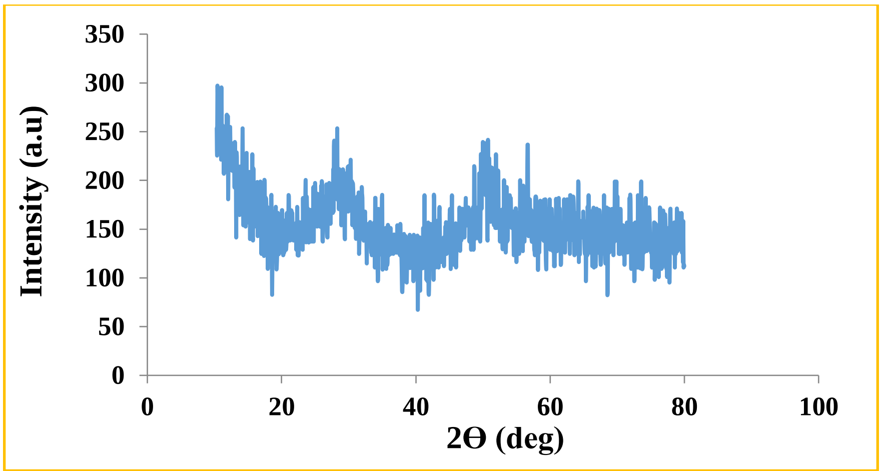

Figure 1: XRD pattern of TeO_2-V_2O_5

3.2 Infrared Absorption Spectra

TeO_2-V_2O_5 glasses were used to study the infrared absorption spectra, which are displayed in **Figure (2)**.

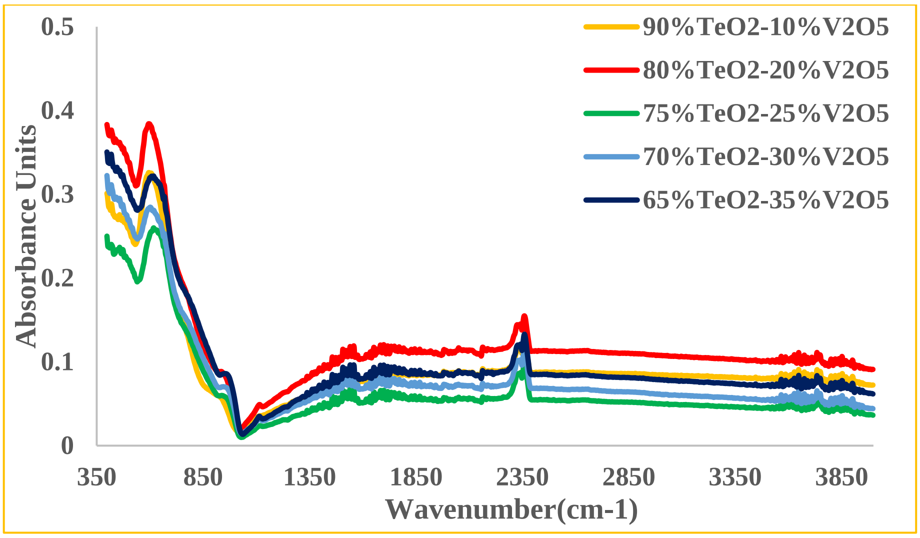

Figure 2: IR spectra of all the studied glass samples

We notice from **Table (1)** that there are many bands in different regions of the infrared range with an increase in the percentage of (V_2O_5), The presence of a band at (541-531) cm-1 could indicate a bend in the Te-O-Te bonds and the triangular expansion of TeO_4 with oxygen bonds, while the bands at (925-928) cm-1 could be due to such vibrations in the bonds V-O where V_2O_5 has strong vibrations in this spectral range **[11]**, while the presence of bands at (1013-1037)cm-1 indicates the vibrations of isolated vanadium groups V=O in (VO_5) trigonal, and the presence of bands at (1582-1642)cm-1 Refers to vibrations in the hydroxyl groups (OH) in the sample, where the bends of the O-H vibrations appear at this spectral range in the form of broadband, while the beams at (3662) cm-1 are due to the retention of water molecules within the structure of the sample **[12]**.

Table 1: Band positions of IR spectra of the studied glass sample

V_2O_5 Content	Band Position (cm^{-1})				
	500	**900**	**1000**	**1500**	**3000**
10	531		1013	1582	3662
20	532		1014	1585	3662
25	541	925	1030	1642	3662
30	540	925	1035		3661
35	541	928	1037		3662

3.3 Raman spectroscopy

Raman spectra were measured for the glass compound (TeO_2-V_2O_5) and all percentages (V_2O_5) at room temperature. **Figure (3.3)** shows the locations of the absorption bands for the Raman spectra. **Table (3)** also shows the values of the absorption bands for the Raman spectra for the glassy compound (TeO_2-V_2O_5).

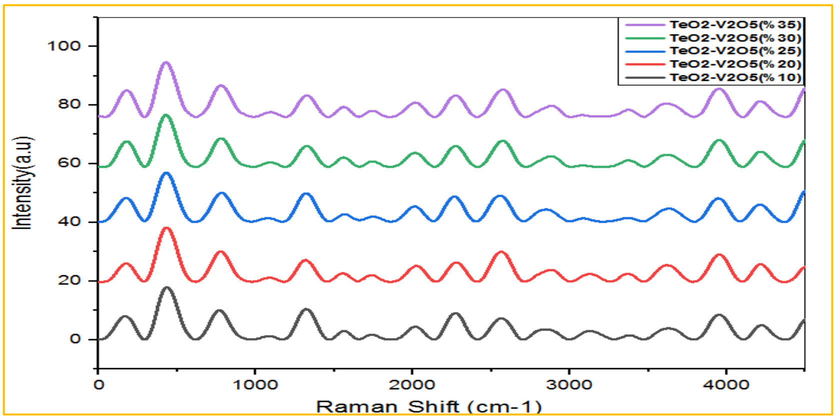

Figure 3: Raman spectra for the glassy compound (TeO_2-V_2O_5)

Table (2) shows the values of the Raman bands for all ratios of (V_2O_5), as we note that there is a band at (433-425) cm-1, which is due to the vibrations in the Te-O-Te bonds in the structural units of TeO_4, and this band represents the peak of the Te-O bonds and V-O vibrations **[12]**, while the bands at (781-768) cm-1 can indicate vibrations in the O-V-O and V=O bonds. When the concentration of V_2O_5 increases, we notice an overlap in the Te-O, V-O bonds, and finally the bands at (1322-1319)cm-1 It indicates the increase of O-V-O and V-O-V groups and the breaking of TeO_2 chains to be replaced by V_2O_5 as the basic network in the glassy group **[13]**.

Table 2: The values of the absorption bands of the Raman spectra for all ratios (V_2O_5) in the glassy compound (TeO_2-V_2O_5)

V2O5 Content	Raman Shift (cm-1)		
10	433	768	1319
20	430	775	1317
25	428	781	1319
30	428	778	1322
35	425	778	1322

3.4 Optical absorption edge

Ultraviolet and visible absorbance measurements were made for the semiconductor glass (TeO_2-V_2O_5) and all percentages (V_2O_5) as a function of wavelength as shown in **Figure (4).**

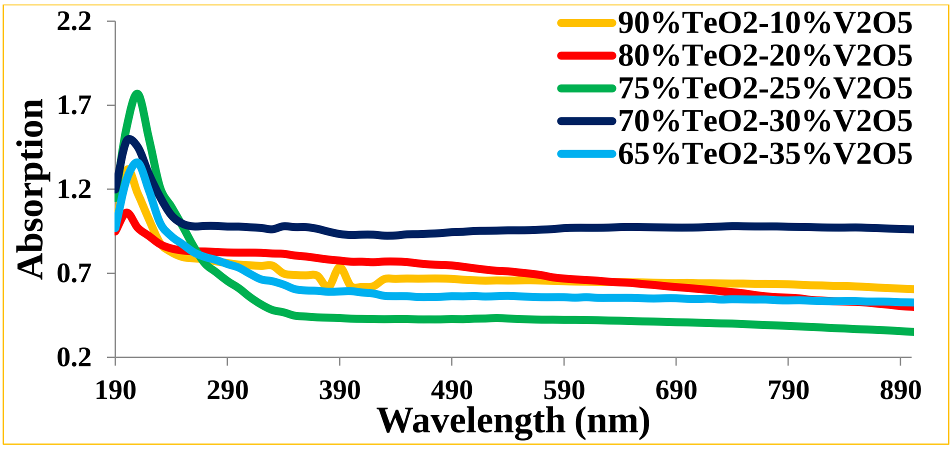

Figure 4: Absorption spectra for all the studied samples

The value of the optical energy gap (E_{opt}) was calculated from the **Figure (5).** The energy of the tail beam (Eo) was calculated from the graph **Figure (6)** between the logarithm of the absorption coefficient (Lnα) with the energy of the incident photon (ħω). the refractive index (n), of the semiconductor glass (TeO_2-V_2O_5) and the absence of sharp absorption edges from the UV-visible absorption spectra confirm the amorphous nature of the glass samples **[14]**.

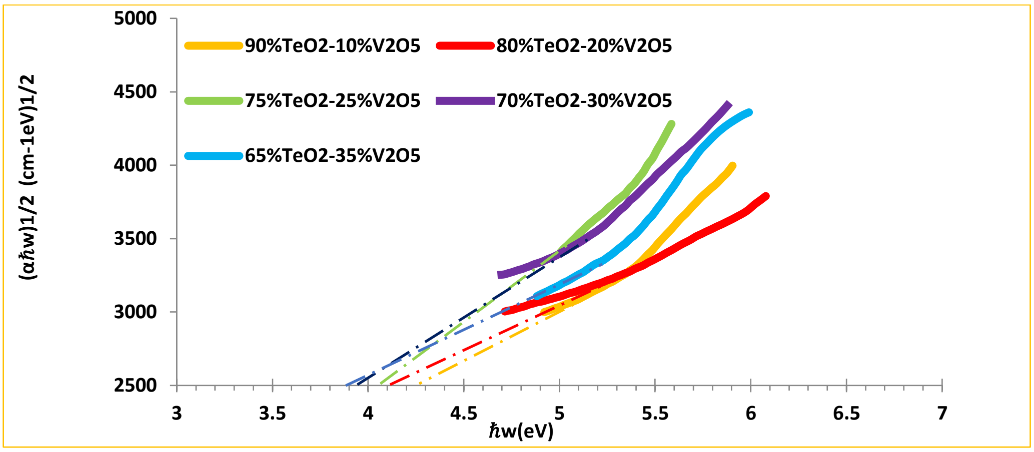

Figure 5: Quantity of $(\omega\hbar\alpha)^{1/2}$ as a function of photon energy in the glassy compound (TeO_2-V_2O_5)

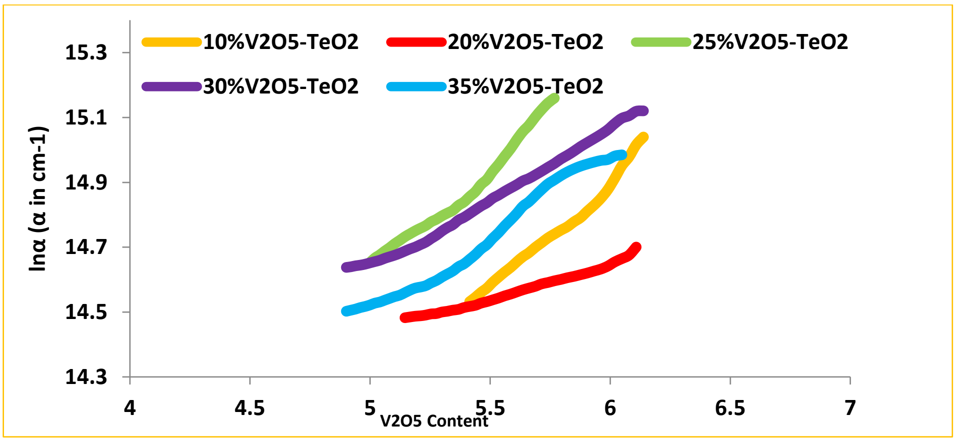

Figure 6: The quantity (lnα) as a function of the photon energy in the glassy compound (TeO_2-V_2O_5)

With the increase in the concentration of (V_2O_5), we notice a decrease in the optical gap energy (E_{opt}) values (4.23-3.93 eV) through the transformation of TeO_2 units into TeO_3 and TeO_4 units, and the establishment of bridging bonds of oxygen as shown in **Figure (7) [15]**, as well as with an increase The concentration of (V_2O_5) in the glass compound, we notice a decrease in the value of the energy of the tail of the band (E_o) (1.5-0.84 Ev), causing a sharp decrease in the long-term arrangement of atoms through the presence of the Te-O-V bridge bonds, which leads to an increase in the number of oxygen bonds, as indicated by The amorphous nature of the glass is consistent with the (XRD) results, which indicate the presence of a periodic three-dimensional network in the glass samples as shown in **Figure (8) [16]**.

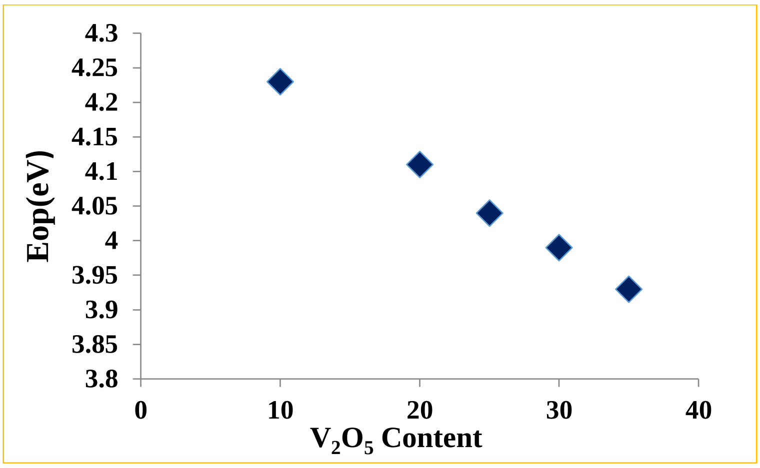

Figure 7: Optical gap energy as a function of (V_2O_5) content in the glass compound (TeO_2-V_2O_5)

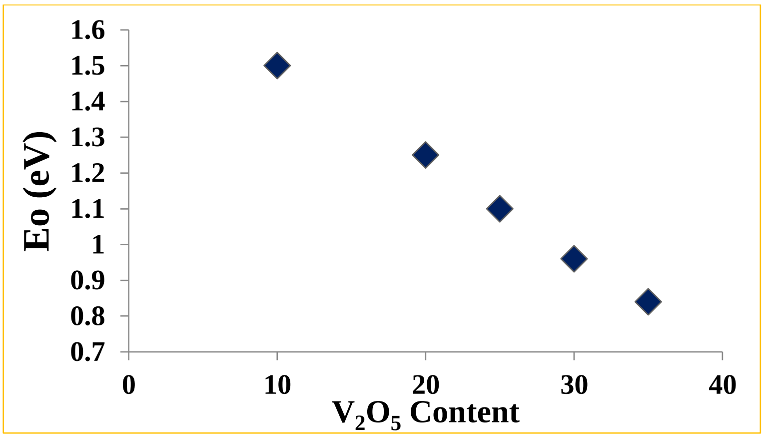

Figure 8: The tail energy of the beam as a function of (V_2O_5) content in the glassy compound (TeO_2-V_2O_5)

Figure (9) shows the increase in the refractive index with an increase in the concentration of (V_2O_5) from (1.80-1.83), as this can be linked to a decrease in unbridged oxygen bonds and an increase in the density of glass samples **Table (3)** shows all Parameters was calculated from UV-Visible spectrum **[17]**.

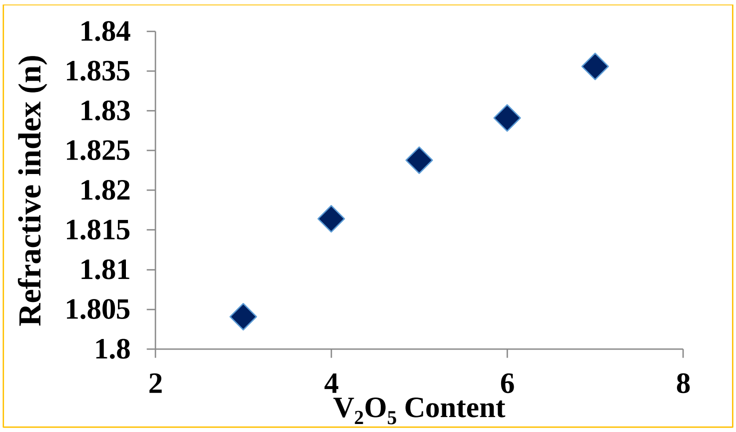

Figure 9: Refractive index as a function of the (V_2O_5) content in the glass compound (TeO_2-V_2O_5)

Table (3) The values of the optical gap energy, band tail energy, and refractive index for all (V_2O_5) content in the glassy compound (TeO_2-V_2O_5)

V205 Content	Eop(Ev)	Eo(Ev)	Refractive Index (n)
10	4.23	1.5	1.804
20	4.11	1.25	1.816
25	4.04	1.1	1.823
30	3.99	0.96	1.829
35	3.93	0.84	1.835

3.5 Differential scanning calorimetry (DSC)

DSC measurements were made for the glassy semiconductor compound (TeO_2-V_2O_5) and all percentages of (V_2O_5) in the compound as shown in **Figure (10)**, where the heat coefficients shown in **Table (4)** were found from the (DSC) curves.

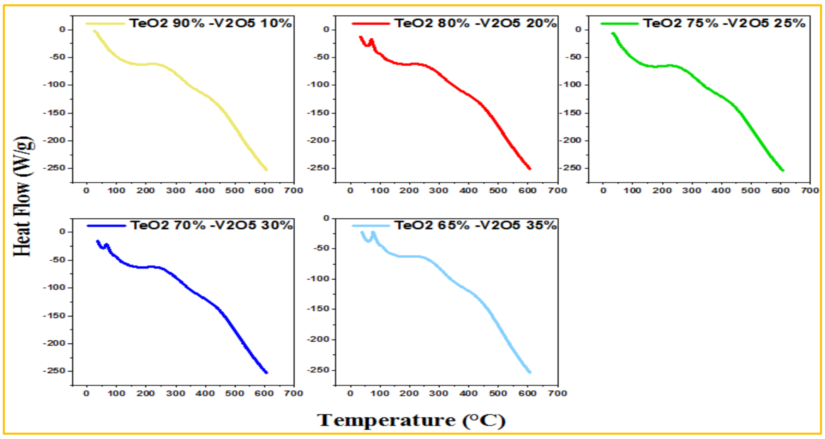

Figure 10: DSC curves for the glass compound (TeO_2-V_2O_5)

Table (4) shows the value of glass transition temperature (Tg), crystallization (Tc), melting temperature (Tp), thermal stability coefficient (ΔT), thermal stability (S), and thermodynamic brittleness (F) for the glass compound (TeO_2-V_2O_5)

V2O5 Content	Tg	Tc	Tp	ΔT	F	S
10	240	355	440	115	0.266247379	40.72916667
20	247	356	442	109	0.237109641	37.951417
25	252	360	444	108	0.226455231	36
30	258	363	448	105	0.199482743	34.59302326
35	266	368	450	102	0.161437701	31.44360902

Table (4) shows an increase in the value of the glass transition temperature (Tg) from 240C° to 266C° with an increase in the percentage of (V_2O_5) in the glass compound from 10mol% to 35mol% as shown in **Figure (11)** where it can be attributed to the increase in (Tg) The V-O bonds contain a higher heat content (644Kj/mol) compared to the heat content of the Te-O bonds (376Kj/mol) and also the arrangement of V_2O_5 atoms inside the glass lattice **[18]**, causing a decrease in the lattice hardness., the increase in (Tc) (368-355)C° with the increase in the concentration of (V_2O_5) is due to the decrease in the spacing between the V_2O_5 atoms, and the values of the thermal stability coefficient (ΔT) range between (102-115)C°, **Figure (12)**, which indicates The prepared glass is good for uses in optical techniques and devices, as the higher (ΔT) the better the quality of the formed glass **[19]**.

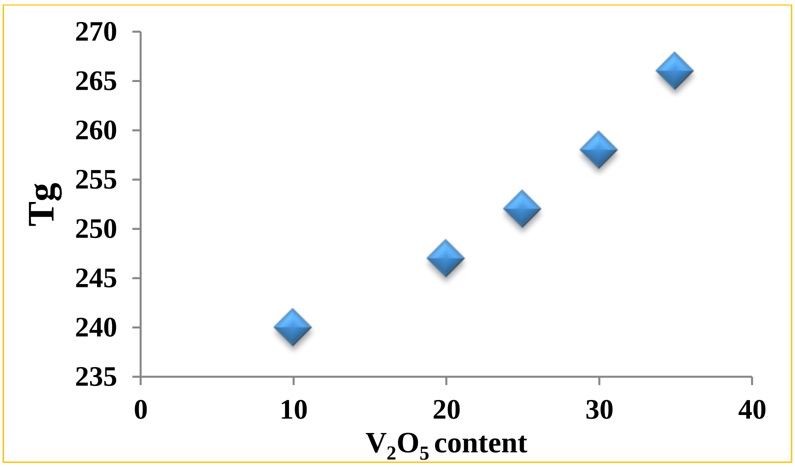

Figure 11: The change in the value of (Tg) as a function of (V_2O_5) content in the glass compound (TeO_2-V_2O)

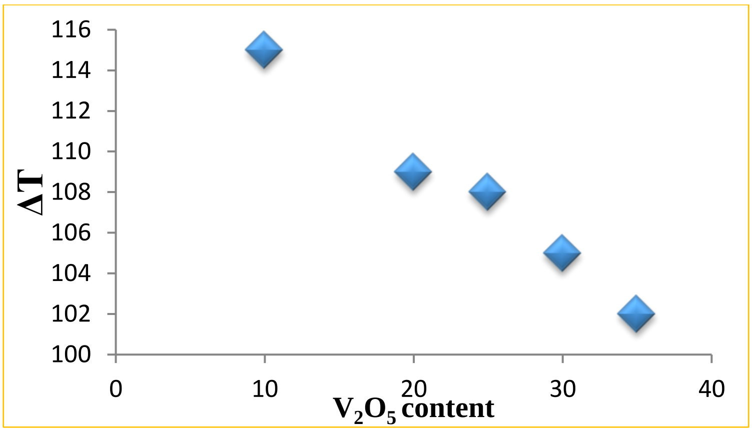

Figure 12: The change in the value of (ΔT) as a function of (V2O5) content in (TeO_2-V_2O_5) composite

The values of the thermal stability coefficient (S) decrease from 40.72 to 31.44 with the increase in the concentration of (V_2O_5) as shown in **Figure (13)**, and the thermodynamic fragility also decreases from 0.266 to 0.161 with the increase in the concentration of (V_2O_5) as shown in the **Figure (14)** due to the formation of bonds of bridging oxygen, which causes more openness in the vitreous lattice with less disturbances **[20]**.

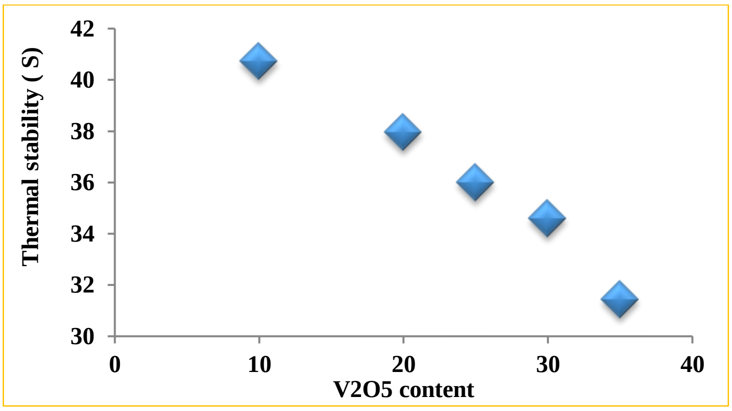

Figure 13: Variation of (S) values as a function of (V_2O_5) content in the glass compound (TeO_2-V_2O_5)

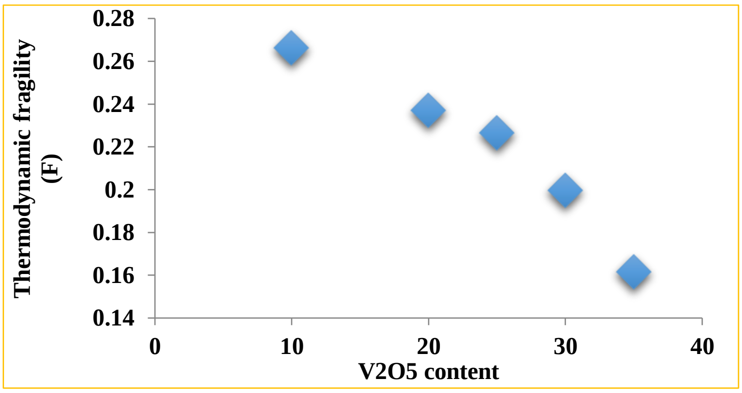

Figure 14: Variation of (F) values as a function of (V_2O_5) content in the glass compound (TeO_2-V_2O_5)

3.6 Scanning electron microscopy (SEM)

Scanning electron microscope measurements were made for the semi-conductive glass compound (TeO_2-V_2O_5) and all ratios (V_2O_5) and with different scales. The samples were measured individually for all scales, but we will suffice in our study with one image for each sample, as shown in **Figure (15)**.

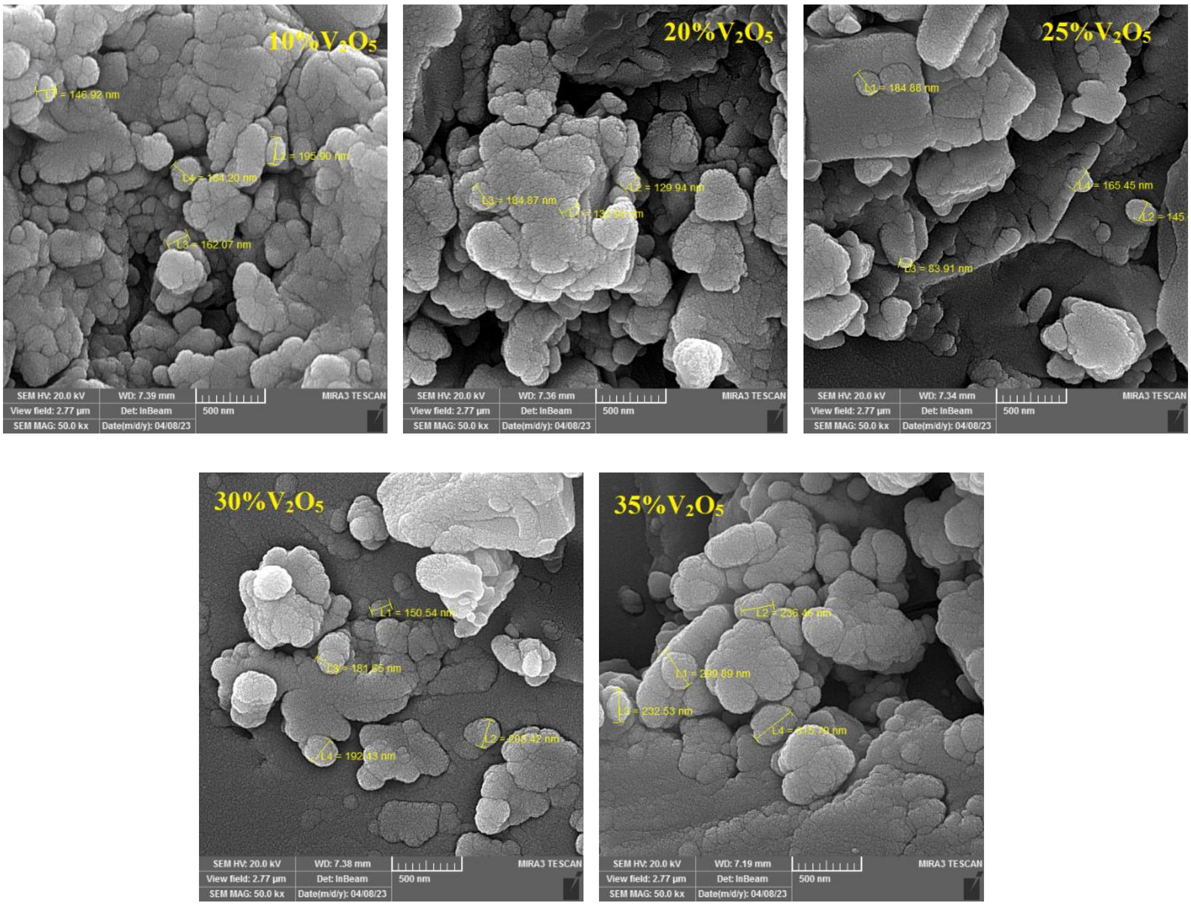

Figure 15: SEM images of all ratios of (V_2O_5) in the glass compound (TeO_2-V_2O_5)

(SEM) images show the glass samples in different shapes and sizes, including nanoparticles, which are shown in a network-shaped structure with ramified structures that extend over the surface of the sample **[21]**. It is well integrated after heat treatment and melting of the material and its fusion is ideal, forming a three-dimensional porous structure that extends over the entire sample distance, and The nanostructure consists of granules well connected and randomly arranged inside the sample, which confirms the amorphous nature of the banned glass **[22,23]**.

4-Conclusion

The X-Ray phase shows that the glass system (TeO_2-V_2O_5) was non-crystalline which mean it is amorphous. The DSC spectra show that the (Tg), and (Tc), increase with rising content of

V_2O_5 from (5% to 25%), thermal stability and thermodynamic fragility decrease with rising content of V_2O_5, and the results of UV-Visible measurements show the following:

1-The (E_{opt}) decreased from (4.23 - 3.93) eV with increasing of V_2O_5 content.

2-The Urbach energy (Eo) decreased from (1.5 - 0.84) eV with increasing of V_2O_5 content.

3-The refractive index (n) is increasing from (1.804 - 1.835) with increasing of V_2O_5 content.

Raman and IR spectrum considered the amorphous structure of glass system (TeO_2-V_2O_5) from the band position and peaks.

5. References

[1] Sreedhar VB, Ramachari D, Jayasankar CK. Optical properties of zincfluorophosphate glasses doped with Dy3+ ions. Physica B: Condensed Matter. 2013 Jan 1;408:158-63.

[2] El-Batal HA, Ezz-El-Din FM. Interaction of γ-rays with some alkali-alkaline-earth borate glasses containing chromium. Journal of the American Ceramic Society. 1993 Feb;76(2):523-9.

[3] M. Abdel-Baki, and F. El-Diasty, Role of oxygen on the optical properties of borate glass doped with ZnO, Journal of Solid State Chemistry, 184, 2762(2011).

[4] B.Sumalatha, I.Omkaram, T.Rao, and C.Raju, The effect of V2O5 on alkaline earth zinc borate glasses studied by EPR and optical absorption, Journal of Molecular Structure Volume 1006, Issues 1–3, 2011, Pages 96-103

[5] Rao RB, Veeraiah N. Study on some physical properties of Li2O–MO–B2O3: V2O5 glasses. Physica B: Condensed Matter. 2004 May 1;348(1-4):256-71.

[6] Guery G, Fargues A, Cardinal T, Dussauze M, Adamietz F, Rodriguez V, Musgraves JD, Richardson K, Thomas P. Impact of tellurite-based glass structure on Raman gain. Chemical Physics Letters. 2012 Dec 3;554:123-7.

[7] W.Vogel in, "Glass Chemistry" 2nd edu, 166,Berlin Springer-velag,(1994), Book.

[8] Kaur R, Kaur R, Khanna A, González F. Structural and thermal properties of vanadium tellurite glasses. InAIP Conference Proceedings 2018 Apr 10 (Vol. 1942, No. 1). AIP Publishing.

[9] Hussain NS, Cardoso PJ, Hungerford G, Gomes MJ, Ali N, Santos JD, Buddhudu S. Physical and optical characterization of Er3+ doped Lead-zinc-borate glass. Journal of Nanoscience and Nanotechnology. 2009 Jun 1;9(6):3555-61.

[10] Dayanand C, Sarma RV, Bhikshamaiah G, Salagram M. Optical properties of lead phosphate glasses. Journal of non-crystalline solids. 1994 Jan 1;167(1-2):122-6.

[11] An Obed S, A Hassan M. A Study of Infrared Spectra of Some Semiconducting Oxide Glasses. Kirkuk University Journal-Scientific Studies. 2016 Sep 28;11(3):100-14.

[12] Abd Hassan M, M Mohammed Ali A. A Study of Optical Properties of Phosphate and Tellurite Semiconducting Oxide Glasses. Kirkuk University Journal-Scientific Studies. 2016 Mar 28; 11(1):224-33.

[13] Saddeek YB, Yahia IS, Dobrowolski W, Kilanski L, Romčević N, Arciszewska M. Infrared, Raman spectroscopy and ac magnetic susceptibility of Gd2O3-TeO2-V2O5 glasses. optoelectronics and advanced materials-rapid communications. 2009 Jun 15;3(June 2009):559-64.

[14] Elkhoshkhany N, Khatab MA, Kabary MA. Thermal, FTIR, and UV spectral studies on tellurite glasses doped with cerium oxide. Ceramics International. 2018 Feb 15;44(3):2789-96.

[15] Dimitrov V, Sakka S. Electronic oxide polarizability and optical basicity of simple oxides. I. Journal of Applied Physics. 1996 Feb 1;79(3):1736-40.

[16] Hossain MK, Hossain S, Ahmed MH, Khan MI, Haque N, Raihan GA. A review of optical applications, prospects, and challenges of rare-earth oxides. ACS Applied Electronic Materials. 2021 Sep 8;3(9):3715-46.

[17] Hussein KI, Al-Syadi AM, Alqahtani MS, Elkhoshkhany N, Algarni H, Reben M, Yousef ES. Thermal Stability, Optical Properties, and Gamma Shielding Properties of Tellurite Glass Modified with Potassium Chloride. Materials. 2022 Mar 24;15(7):2403.

[18] Elkhoshkhany, N., and Eslam Syala. "Kinetic characterization of TeO2–Bi2O3–V2O5–Na2O–TiO2 glass system." Ceramics International 43.8 (2017): 6156-6162.

[19] A. Abd El-Moneim DTA and IR absorption spectra of vanadium tellurite glasses Materials Chemistry and Physics 73 (2002) 318–322

[20] Souri, Dariush. "Fragility, DSC and elastic moduli studies on tellurite vanadate glasses containing molybdenum." Measurement 44.10(2011): 1904-1908.

[21] Przemysław Sielicki1*, Helena Janik1, Agnieszka Guzman1, Alan Reynolds2, Jacek Namieśnik, Analysis of airborne metal-containing particles with DX/EDS detectors in electron microscopes Cent. Eur. J. Chem. • 9(2) • 2011 • 308-313

[22] Sozan Abd-allah Hassan, Novel Hydrothermal synthesis and characteristics of thin films V2O5@TeO2with CTAB for detection of NO2 gas Invention Journal of Research Technology in Engineering & Management (IJRTEM) ISSN: 2455-3689, Volume 3 Issue 5 ǁ July –August 2019 ǁ PP 49-58

[23] Chen Y, Shi Y, Xie J, Lei F, Fan L, Zhang L. Fabrication of lead-free low melting temperature TeO2-V2O5-CuO glasses and wetting behavior on AlN ceramic substrate. Journal of the European Ceramic Society. 2020 Dec 1;40(15):5991-6001.